# Heavy Ions and Anisotropies as in-situ Diagnostics of Solar Wind and Coronal Heating

Aidan Nakhleh[1], Nicholeen Viall[2], Susan Lepri[1], and Jim Raines[1]

[1]University of Michigan, [2]NASA Goddard Spaceflight Center

Contact: naidan@umich.edu

Check out our paper! https://doi.org/10.1029/2025JA034762

Interested in solar wind formation and structure? Follow orange headers

Interested in solar wind kinetic processes and heating? Follow blue headers

# Introduction

## Heavy Ions in the Solar Wind

- The solar wind is composed of ~96% protons, ~4% alpha particles, and <0.1% ionized heavy elements (C, O, Ne, Mg, Si, Fe, etc.) by number.
- Like leaves on a stream, heavy ion properties reveal processes occurring in the corona and the solar wind.
  - Densities of ions in different charge states set deep in the corona via the "freeze-in effect" probe solar wind source regions **[1]**.
  - Abundance ratios probe the First Ionization Potential (FIP) effect **[2]**.
  - Super mass-proportional heavy ion temperatures and differential streaming probe solar wind heating from resonant absorption **[3, 4]** and kinetic Alfvén wave (KAW) turbulence **[5,6]**.
- Outstanding questions in Heliophysics relate to the formation of the solar wind and physical mechanisms operating on solar wind formation/evolution **[7]**.
- **We can utilize heavy ion properties measured by ACE/SWICS to help in efforts to answers to these questions.**

# Methodology

## On Solar Wind Release

- Proton specific entropy, $S = k_B \ln(T_p^{3/2}/n_p)$, is strongly correlated with $O^{7+}/O^{6+}$ **[8]**.
  - Large-scale energization signatures appear preserved from the corona into the solar wind.

**Where is solar wind entropy variability set in the corona?**

➢ Method: cross-correlate other heavy ion properties with entropy.

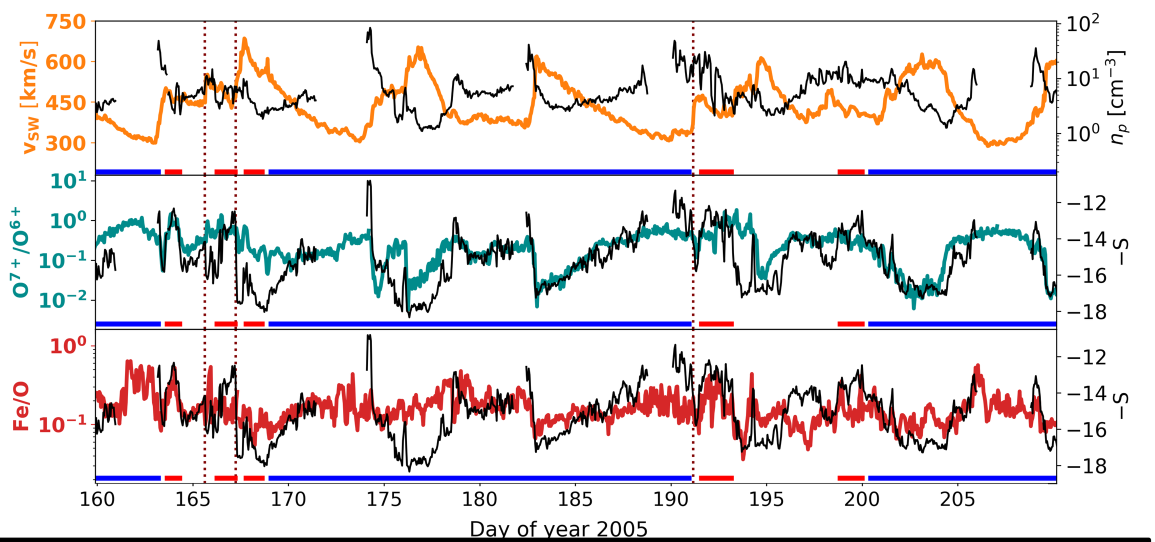


**Fig 1.** Time series of $O^{7+}/O^{6+}$ and Fe/O plotted against **entropy (S)** over a wide range of solar wind conditions. ICME times **[9]** are marked in bright red and maroon dashes represent shocks **[10]**, both of which are excluded from our analysis.

## On Solar Wind Heating

- Heavy ions are heated super-mass-proportionally **[11]** and can stream faster than protons along $\vec{B}$ **[12,13]**.
  - If ion-gyroscale turbulent fluctuations stochastically heat ions, differential streaming should regulate $T_{\perp i}/T_{\perp p}$ **[6]**.

**Does the super-mass-proportionality of ion temperatures change with differential streaming magnitude?**

➢ Method: organize 11 heavy ion-proton temperature ratios by Helium field-aligned differential streaming speed: $\Delta V_{\alpha p} = -\cos\theta_{\vec{B},\vec{v}_p} + \mathrm{sgn}\{\cos\theta_{\vec{B},\vec{v}_p}\}\sqrt{V_\alpha^2 - V_p^2 \sin^2\theta_{\vec{B},\vec{v}_p}}$

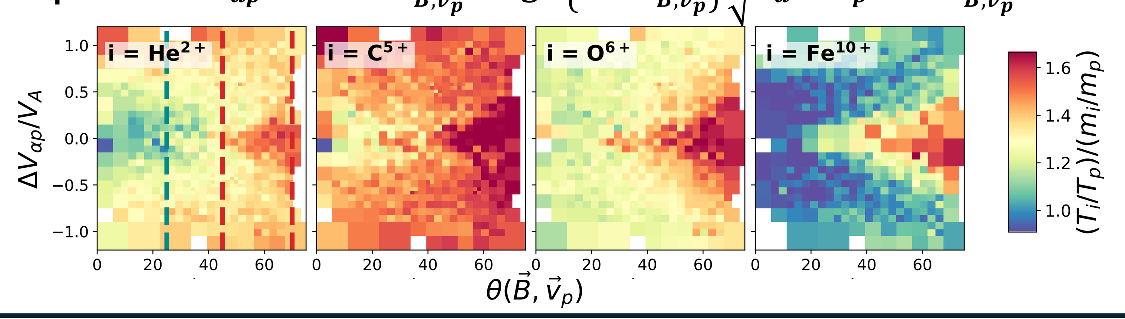


**Fig 2.** Reconstructed Helium field-aligned differential streaming ($\Delta V_{\alpha p}/V_A$) **[12]** vs solar wind velocity-IMF angle ($\theta_{\vec{B},\vec{v}_p}$), color-coded to the ion-proton temperature ratio normalized to the ion mass for four heavy ions measured by ACE/SWICS. Only low collisional age solar wind data ($A_{C,i-p} < 0.1$) is used. As $\theta_{\vec{B},\vec{v}_p} \to 90°$, components of the velocity distribution preferentially perpendicular to the IMF are expected to be observed by ACE/SWICS. Data between the dashed red lines ($45° < \theta_{\vec{B},\vec{v}_p} < 70°$*) are used for the subsequent analysis of perpendicular heating.

# Observations

## Entropy Variability Stops Evolving in the Middle Corona

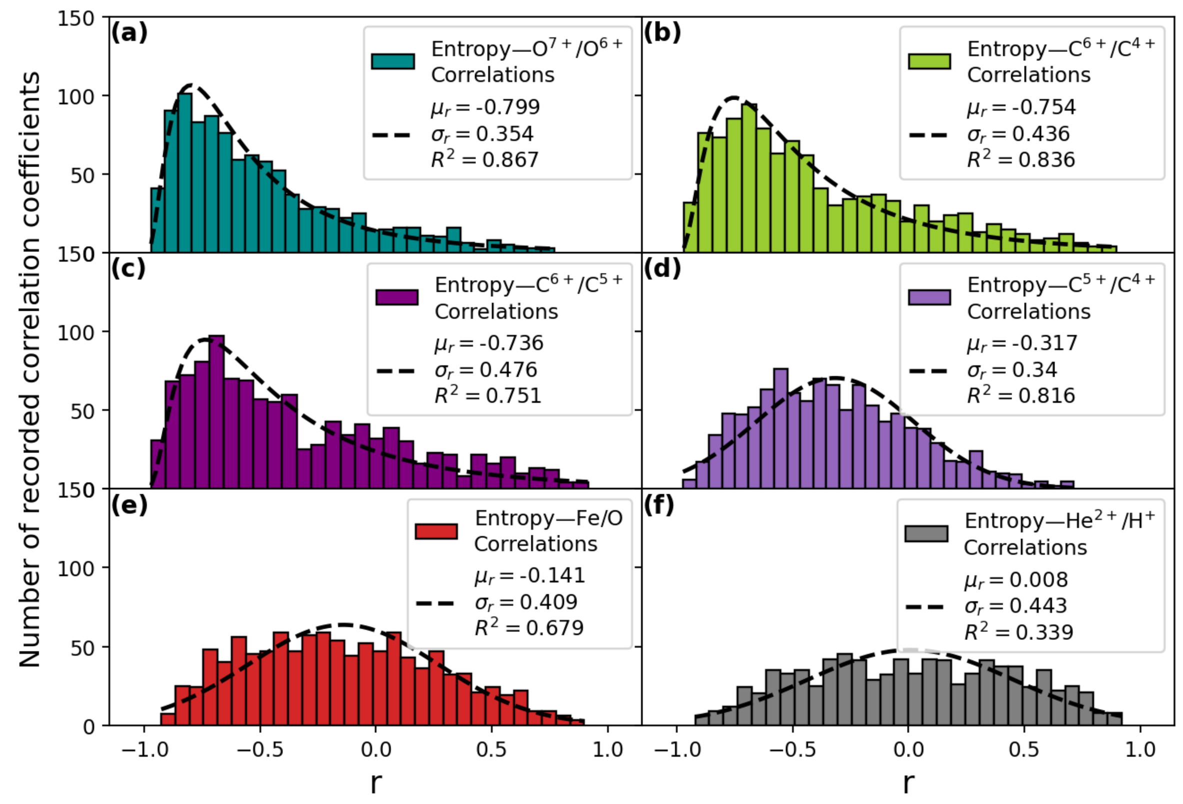


**Fig 3.** Distributions of correlation coefficients between entropy and six selected heavy ion distribution properties over two-day sampling periods spanning 1998-2011 excluding ICMEs, along with log-normal fits in panels a,b,c, and normal fits in panels d,e,f.

## Differential Streaming Regulates $T_{\perp i}/T_{\perp p}$

$$\frac{T_{\perp i}}{T_{\perp p}} = A_i \left(\frac{A_i}{Z_i}\right)^{\frac{2a}{1-a}} \frac{\left\langle \chi^{\frac{1}{1-a}} \right\rangle_i}{\left\langle \chi^{\frac{1}{1-a}} \right\rangle_p} \quad \text{Eq. (1)}$$

$$\left\langle \chi^{\frac{1}{1-a}} \right\rangle_i = \frac{1}{\sqrt{\pi} w_{\parallel i}} \int_{-\infty}^{\infty} dv_\parallel \chi^{\frac{1}{1-a}} \exp\left(-\frac{(v_\parallel - \Delta V_{ip})^2}{w_{\parallel i}^2}\right) \quad \text{Eq. (2)}$$

$$\chi = \frac{2}{r_A + 1}\left(r_A + \frac{v_\parallel^2}{v_A^2}\right) - \frac{2\sigma v_\parallel}{v_A} \quad \text{Eq. (3)}$$

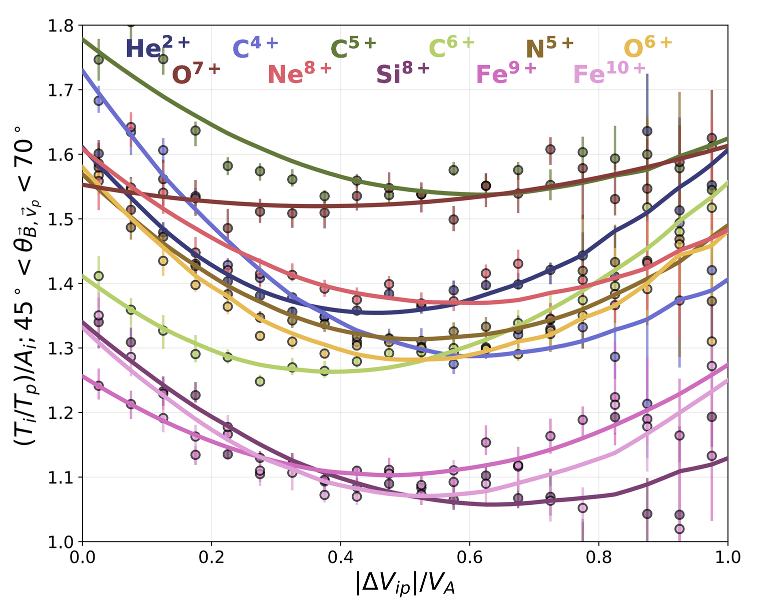


**Fig 4.** Median $T_i/T_p$ vs $|\Delta V_{ip}/V_A|$ for the 11 highest-abundance solar wind heavy ions. To obtain quasi-perpendicular temperatures, only $45° < \theta_{\vec{B},\vec{v}_p} < 70°$ data are used*. Each ion curve is fitted to Eq. (1) producing 11 sets of free parameters $a$, $\sigma$, and $r_A$.
$\mathbf{med}(a) = 0.2$
$\mathbf{med}(\sigma) = 0.5$
$\mathbf{med}(r_A) = 1.2$

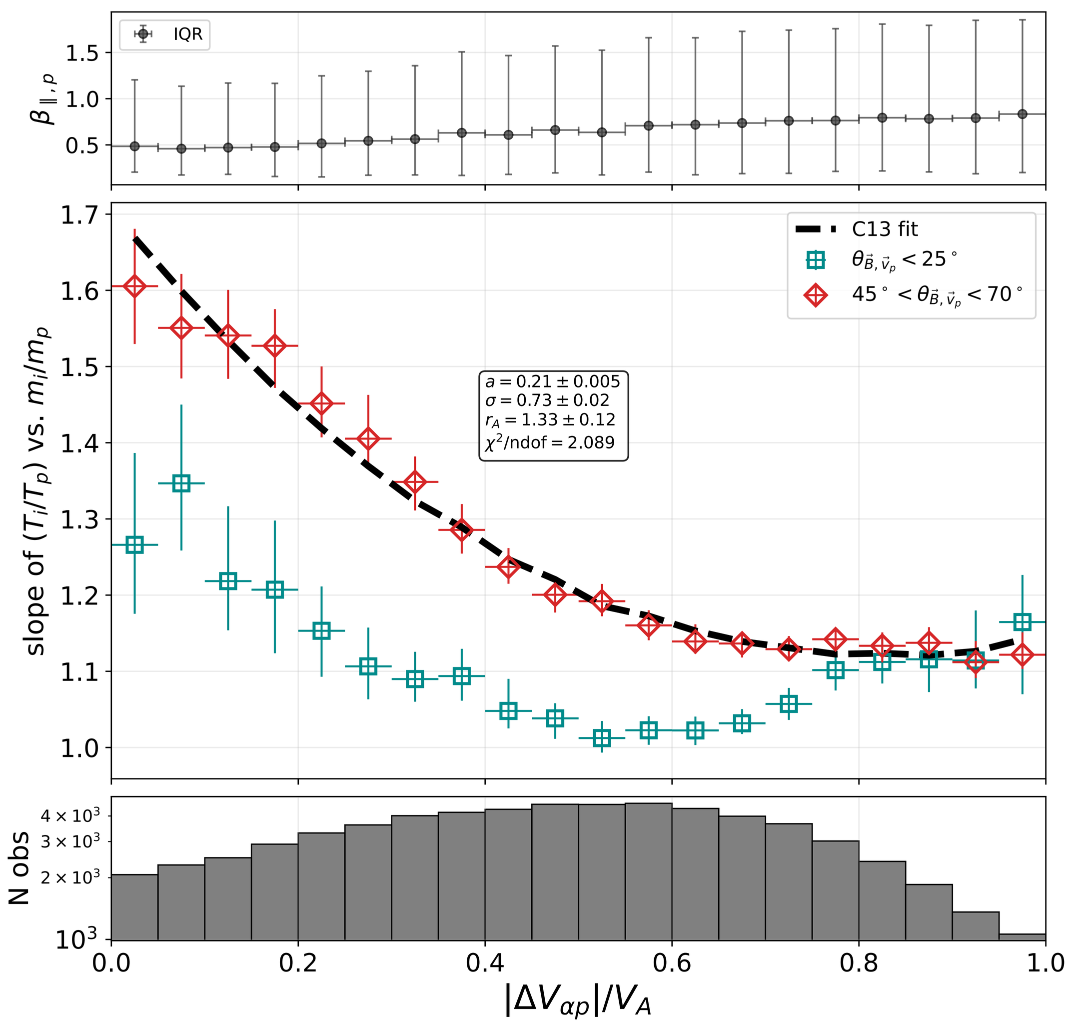


**Fig 5.** Slopes of linear fits between median $T_i/T_p$ and $m_i/m_p$ for 20 different Helium differential streaming bins, along with bootstrapped slope uncertainties. **Red diamonds** correspond to preferentially perpendicular temperature ratios (i.e. $T_i/T_p \approx T_{\perp i}/T_{\perp p}$, while **blue squares** correspond to preferentially parallel temperature ratios (i.e. $T_i/T_p \approx T_{\parallel i}/T_{\parallel p}$). Also included is a fit from the theory of stochastic ion heating by turbulence **[6]**, which predicts a relationship between $T_{\perp i}/T_{\perp p}$ and $\Delta V_{ip}/V_A$. The free parameters fitted are the **fluctuation energy exponent $a$**, the **fractional cross helicity $\sigma$**, and the **gyroscale Alfvén ratio $r_A$**.

*For $\theta_{\vec{B},\vec{v}_p} > 70°$, uncertainties in the reconstructed differential streaming become significant **[12]**.

# References

[1] Hundhausen et al., 1968. https://doi.org/10.1086/180165
[2] Laming et al., 2019. https://doi.org/10.3847/1538-4357/ab23f1
[3] Hollweg et al. 2002. https://doi.org/10.1029/2001JA000270
[4] Kasper et al. 2013. https://doi.org/10.1103/PhysRevLett.110.091102
[5] Kasper et al., 2008. https://doi.org/10.1103/PhysRevLett.101.261103
[6] Chandran et al. 2013. https://doi.org/10.1088/0004-637X/776/1/45
[7] Viall & Borovsky, 2020. https://doi.org/10.1029/2018JA026005
[8] Pagel et al., 2004. https://doi.org/10.1029/2003JA010010
[9] Cane & Richardson, 2024. https://izw1.caltech.edu/ACE/ASC/DATA/level3/icmetable2.htm
[10] Stevens & Kasper, 2014. https://lweb.cfa.harvard.edu/shocks/
[11] Tracy et al., 2016. https://doi.org/10.1103/PhysRevLett.116.255101
[12] Berger et al. 2011. https://doi.org/10.1103/PhysRevLett.106.151103
[13] Rivera et al. 2025. https://doi.org/10.3847/2041-8213/adfa97
[14] Landi & Lepri, 2015. https://doi.org/10.1088/2041-8205/812/2/L28
[15] Cranmer et al., 2007. https://doi.org/10.1086/518001
[16] Bale et al., 2005. https://doi.org/10.1103/PhysRevLett.94.215002
[17] Holmes et al., 2024. https://doi.org/ 10.3847/1538-4357/ad23ea

# Discussion

## Heavy Ion Densities Probe Coronal Thermodynamics

| Charge state ratio | CH freeze-in distance($R_\odot$) | HS freeze-in distance($R_\odot$) | AR freeze-in distance($R_\odot$) |
|---|---|---|---|
| $O^{7+}/O^{6+}$ | 1.72 | 1.68 | 1.50 |
| $C^{6+}/C^{4+}$ | 1.68 | 1.75 | 1.64 |
| $C^{6+}/C^{5+}$ | 1.52 | 1.67 | 1.67 |
| $C^{5+}/C^{4+}$ | 1.45 | 1.62 | 1.48 |

**Table 1.** Heliocentric distances at which ions of carbon and oxygen reach 90% of their frozen-in values calculated with the Michigan Ionization Code (MIC) **[14]**, using self-consistent temperature, density, and velocity profiles associated with coronal holes (CHs), helmet streamers (HSs), and active regions (ARs) developed by **[15]**.

- **Decorrelations between Fe/O and $O^{7+}/O^{6+}$ indicate sudden flux openings — interchange reconnection — in the corona.**
- **Entropy variability evolves after Fe/O is set in the corona, continues to evolve after $C^{5+}/C^{4+}$ freezes-in, and eventually freezes-in along with the other mentioned charge state ratios.**

## Heavy Ion Temperatures Probe KAW Turbulence

- fluctuation energy scaling exponent: $W_i = W_p(\rho_i/\rho_p)^{2a}$ where $W \equiv \frac{1}{4}\langle|\vec{z}^+|^2 + |\vec{z}^-|^2\rangle$
- Gyroscale fractional cross helicity: $\sigma = \frac{\langle|\vec{z}^+|^2 - |\vec{z}^-|^2\rangle}{\langle|\vec{z}^+|^2 + |\vec{z}^-|^2\rangle}$ where $\vec{z}^\pm = \delta\vec{v} \mp v_A \frac{\delta\vec{B}_\perp}{B_0}$ and $\delta\vec{B}_\perp = \delta\vec{B} - \hat{b}(\hat{b}\cdot\delta\vec{B})$
- Gyroscale Alfvén ratio: $r_A = \left(\frac{B_0}{v_A}\right)^2 \frac{\langle|\delta\vec{v}|^2\rangle}{\langle|\delta\vec{B}_\perp|^2\rangle}$
- Least-squares fit gives [1] $a \approx 0.21$, [2] $\sigma \approx 0.7$, and [3] $r_A \approx 1.3$
  - **[1] Only partial cross-field coupling between ions/electrons near $k_\perp\rho_i \gtrsim 1$ [6,16].**
  - **[2] Imbalanced turbulence: $\langle|\vec{z}^+|^2\rangle > \langle|\vec{z}^-|^2\rangle$.**
  - **[3] Slightly more energy in $\vec{E}\times\vec{B}$ velocity fluctuations than $\vec{B}$ fluctuations [6,16].**

# The Big Picture

## Pathways to Solar Wind Release in the Corona

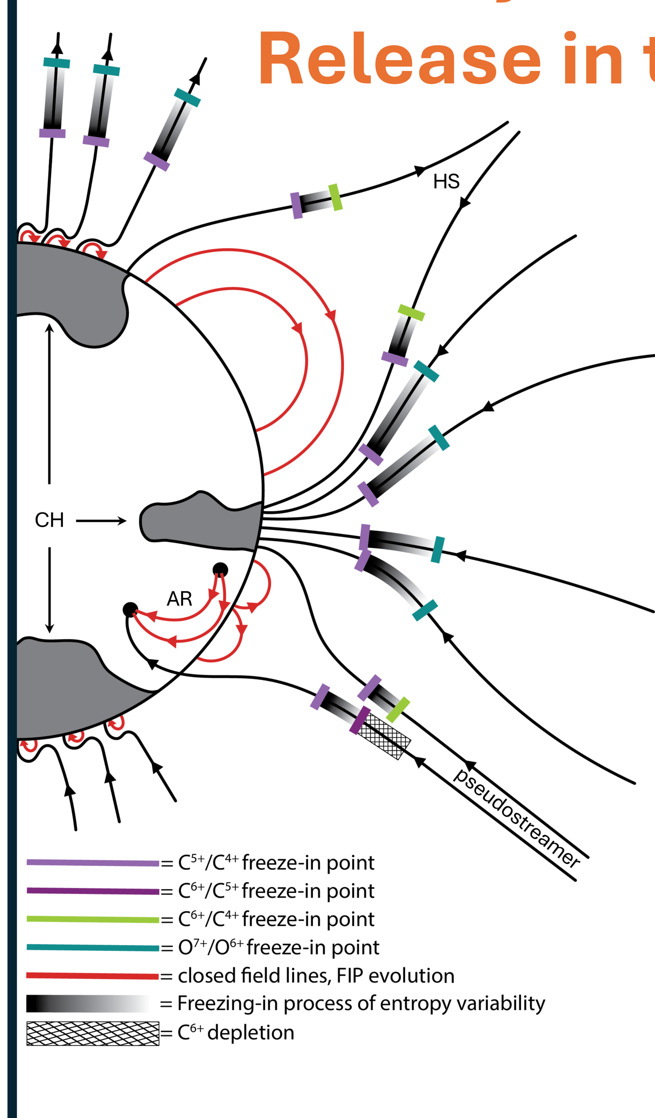


Steady-state calculations of charge state freeze-in heights act as snapshots for **entropy evolution**. Elemental abundance behavior constrains interchange reconnection.

**Fig 6.** Illustration of the decrease in evolution of entropy variability in the solar corona over a range of coronal structures producing solar wind that may be observed by ACE. The region of entropy variability freezing-in is constrained by freeze-in distances of heavy ion charge state ratios calculated using the MIC — a steady-state model.

## Mechanisms for Collisionless Heating in the Solar Wind

Heavy ions may be preferentially heated up to ~100 $R_\odot$, within the reach of Solar Orbiter. **3D Heavy ion VDFs can be constructed.** These measurements may help disentangle **resonant/ stochastic heating processes.**

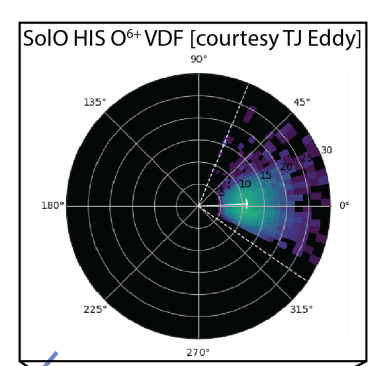


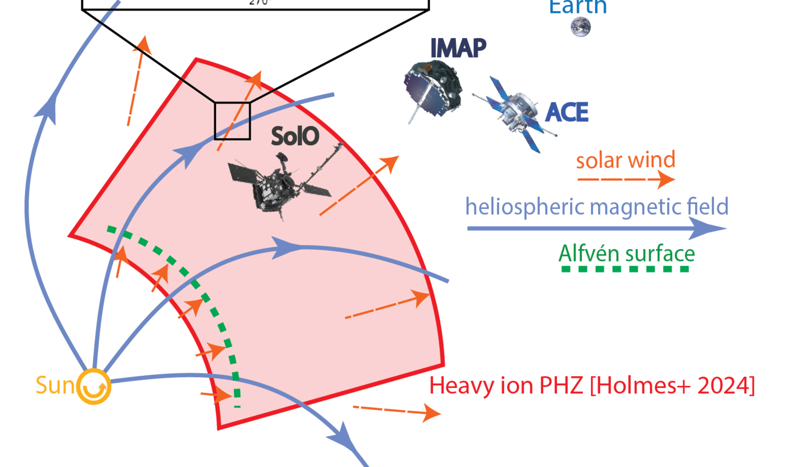


**Fig 7.** Overview of spacecraft with heavy ion instruments in the Heliosphere, along with the hypothesized upper boundary of the preferential heating zone (PHZ) for heavy ions **[17]**. Also included is a collapsed 3D velocity distribution function (VDF) of $O^{6+}$ measured by the Heavy Ion Sensor (HIS) onboard Solar Orbiter (SolO).